



Magnetic Resonance Imaging Tracking of Ferumoxytol-Labeled Human Neural Stem Cells: Studies Leading to Clinical Use

Departments of

^aNeurosciences, ^cPathology, ^eCancer Immunotherapy and Tumor Immunology, and ^hInformation Sciences and ^kDivision of Neurosurgery, City of Hope National Medical Center and Beckman Research Institute, Duarte, California, USA; ^bFrank Laboratory, Radiology and Imaging Sciences, Clinical Center and National Institute of Biomedical Imaging and Bioengineering, NIH, Bethesda, Maryland, USA; Departments of ^dRadiology, ^ePathology, and ^fBiomedical Engineering, CHLA/Keck School of Medicine, University of Southern California, Los Angeles, California, USA; ⁱBrain Tumor Center, University of Chicago Pritzker School of Medicine, Chicago, Illinois, USA; ^jDivision of Neurology, Department of Medicine, UBC Hospital, University of British Columbia, Vancouver, British Columbia, Canada

*Contributed equally as principal investigators.

Correspondence: Rex A. Moats, Ph.D., Dept. of Radiology, 4650 Sunset Blvd., Los Angeles, California 90027, USA. Telephone: 406-650-7120; E-Mail: RMoats@chla.usc.edu; or Karen S. Aboody, M.D., Dept. of Neurosciences, 1500 East Duarte Rd., Duarte, California 91010-3000, USA. Telephone: 626-471-7177; Fax: 626-301-8857; E-Mail: kaboody@coh.org

Received March 13, 2013; accepted for publication May 28, 2013; first published online in *SCTM EXPRESS* September 6, 2013.

©AlphaMed Press
1066-5099/2013/\$20.00/0

<http://dx.doi.org/10.5966/sctm.2013-0049>

MARGARITA GUTOVA,^a JOSEPH A. FRANK,^b MASSIMO D'APUZZO,^c VAZGEN KHANKALDYAN,^{d,e,f} MEGAN M. GILCHRIST,^a ALEXANDER J. ANNALA,^a MARIANNE Z. METZ,^a YELENA ABRAMYANTS,^a KELSEY A. HERRMANN,^a LUCY Y. GHODA,^a JOSEPH NAJBAUER,^a CHRISTINE E. BROWN,^g M. SUZETTE BLANCHARD,^h MACIEJ S. LESNIAK,ⁱ SEUNG U. KIM,^j MICHAEL E. BARISH,^a KAREN S. ABOODY,^{a,k,*} REX A. MOATS^{d,e,f,*}

Key Words. Cell transplantation • Cellular therapy • Clinical trials • In vivo tracking • Neural stem cell • Stem cell • Stem cell transplantation

ABSTRACT

Numerous stem cell-based therapies are currently under clinical investigation, including the use of neural stem cells (NSCs) as delivery vehicles to target therapeutic agents to invasive brain tumors. The ability to monitor the time course, migration, and distribution of stem cells following transplantation into patients would provide critical information for optimizing treatment regimens. No effective cell-tracking methodology has yet garnered clinical acceptance. A highly promising noninvasive method for monitoring NSCs and potentially other cell types in vivo involves preloading them with ultrasmall superparamagnetic iron oxide nanoparticles (USPIOs) to enable cell tracking using magnetic resonance imaging (MRI). We report here the preclinical studies that led to U.S. Food and Drug Administration approval for first-in-human investigational use of ferumoxytol to label NSCs prior to transplantation into brain tumor patients, followed by surveillance serial MRI. A combination of heparin, protamine sulfate, and ferumoxytol (HPF) was used to label the NSCs. HPF labeling did not affect cell viability, growth kinetics, or tumor tropism in vitro, and it enabled MRI visualization of NSC distribution within orthotopic glioma xenografts. MRI revealed dynamic in vivo NSC distribution at multiple time points following intracerebral or intravenous injection into glioma-bearing mice that correlated with histological analysis. Preclinical safety/toxicity studies of intracerebrally administered HPF-labeled NSCs in mice were also performed, and they showed no significant clinical or behavioral changes, no neuronal or systemic toxicities, and no abnormal accumulation of iron in the liver or spleen. These studies support the clinical use of ferumoxytol labeling of cells for post-transplant MRI visualization and tracking. *STEM CELLS TRANSLATIONAL MEDICINE* 2013;2:000–000

INTRODUCTION

Stem cell-based therapies for numerous diseases are currently under clinical investigation, including stem cell-mediated therapy of invasive solid tumors. A first-in-human study of neural stem cell (NSC)-mediated enzyme/prodrug treatment of recurrent glioma is currently in phase I clinical trial (ClinicalTrials.gov identifier NCT01172964) [1]. At present, there is a critical need for a noninvasive technology that would enable monitoring of stem cell migration and distribution over time. Once injected, whether intracerebrally or intravenously, NSCs migrate toward and distribute within distant tumor foci. Several studies have investigated the labeling of stem cells with reporter genes or various contrast agents for noninvasive cell tracking in vivo [2, 3]. For exam-

ple, stem cells have been labeled with fluorescent or bioluminescent reporter genes to enable their visualization in vivo in animal tumor models [4–8]. Although these approaches have been successful in animal models, the limitations of light propagation through human tissues severely restrict the translation of these imaging protocols to the clinical setting. In contrast, the tracking of iron-labeled cells by magnetic resonance imaging (MRI) could potentially be performed clinically in humans to demonstrate stem cell migration, tumor tropism, and tumor distribution and to provide critical information for optimizing treatment regimens and strategies [9].

A particularly promising method for monitoring NSCs, and potentially other cell types, involves preloading the cells with superparamagnetic iron oxide nanoparticles (SPIOs) prior to

administration and subsequently tracking their migration and tumor distribution over time with MRI [10–12]. MRI is the primary method of assessing therapeutic responses in brain tumor patients, and it will facilitate the development of imaging and cell labeling protocols designed in part to track NSCs over time. In previous studies, we demonstrated the effectiveness of MRI to track ferumoxide (Feridex; Berlex Laboratories, Inc., Wayne, NJ, <http://www.berlex.com>)-labeled NSCs in orthotopic glioma-bearing mice [13]. These ferumoxide-labeled NSCs retained their properties of sustained high levels of viability, tumor tropism, and transgene expression, as well as the lack of tumorigenicity and toxicity. Other work has shown the utility of MRI for tracking SPIO-labeled leukocytes and mesenchymal stem cells in preclinical models [14, 15]. The safe use of SPIO MRI contrast agents in patients has been demonstrated for central nervous system (CNS) tumor visualization and for diagnostic MRI purposes following intravenous administration of contrast agents [16, 17]. On the basis of these reports, we hypothesized that SPIO (70–140 nm) or ultrasmall SPIO (17–31 nm) cell labeling can be safely and effectively used in the clinical setting for MRI tracking of NSCs introduced into the brain at the time of tumor biopsy or resection.

Previously, several laboratories showed the off-label utility of Feridex, a U.S. Food and Drug Administration (FDA)-approved dextran-coated SPIO nanoparticle (intravenous iron formulation) used clinically as a contrast agent in patients for MRI detection of liver lesions, but the product was removed from the market in 2009. Since then, the laboratory of Joseph Frank at the NIH has led the way toward developing a labeling and imaging protocol using clinical-grade ferumoxytol (Feraheme; AMAG Pharmaceuticals, Inc., Lexington, MA, <http://www.amagpharma.com>) [18]. Ferumoxytol, a colloidal suspension of carbohydrate-coated ultrasmall superparamagnetic iron oxide nanoparticles (USPIOs) (intravenous iron formulation), is currently approved to treat iron deficiency anemia in patients with chronic kidney disease [19]. The objectives of our current study were (a) to optimize the ratios of heparin, protamine sulfate, and ferumoxytol (HPF) for labeling of NSCs, while maintaining cell viability, growth kinetics, and tumor tropism *in vitro* and *in vivo*; (b) to demonstrate the tracking of HPF-labeled NSCs by MRI *in vivo*; and (c) to demonstrate the acute, midterm, and long-term safety and lack of toxicity of HPF-labeled NSCs administered intracranially in mice for the purpose of advancing this technology to the clinic. These data, *in toto*, support the safety, feasibility, and utility of ferumoxytol labeling for magnetic resonance-based noninvasive cell tracking *in vivo*, and they contributed to FDA approval of this method for the current clinical trial.

MATERIALS AND METHODS

Neural Stem Cell Culture and Iron Labeling

Human HB1.F3.CD NSCs (clone 21, passage 20 from the established Master Cell Bank at City of Hope cGMP facility) were thawed and cultured in T-175 tissue culture flasks in Dulbecco's modified Eagle's media (DMEM) (10313-021; Invitrogen, Carlsbad, CA, <http://www.invitrogen.com>) supplemented with 10% heat-inactivated fetal bovine serum (FBS) (SH30070.03; HyClone, Logan, UT, <http://www.hyclone.com>) and 2 mM L-glutamine (25030-081; Invitrogen). NSCs were incubated (37°C, 6% CO₂) for 72 hours prior to labeling with HPF complex [20, 21]. For

unlabeled NSCs, cells were thawed and incubated for 72 hours and then treated using the same protocol as HPF-labeled cells without HPF complex in the media. After labeling, NSCs were incubated (37°C, 6% CO₂) for an additional 24 hours; the cells were then washed with phosphate-buffered saline (PBS), trypsinized, concentrated to 2.5×10^5 NSCs per 2 μ l of PBS containing heparin (10 U/ml), and injected intracerebrally in 2 μ l of PBS. For intravenous injections, NSCs were cultured and prepared as described for intracerebral injections, except the NSC doses were 5×10^5 or 2×10^6 cells per 200 μ l of PBS containing heparin (10 U/ml).

For iron labeling, the HPF complex was prepared by combining, in order, heparin (2 U/ml), protamine sulfate (40 μ g/ml) (both from American Pharmaceuticals Partners, LLC, Lake Zurich, IL, <http://www.appharma.com>), and ferumoxytol (100 μ g/ml) (Feraheme; AMAG Pharmaceuticals, Inc., Schaumburg, IL, <http://www.amagpharma.com>). The HPF complex was added to NSCs in 10 ml of serum-free culture media in one T-175 tissue culture flask (72 hours after thawing of cells), and NSCs were then incubated (2 hours, 37°C, 6% CO₂). Culture medium (10 ml) supplemented with 20% FBS was then added to the flask (without removing the previous medium) and cells were incubated overnight (37°C, 5% CO₂). After 24 hours, NSCs were washed first with PBS only, then with PBS containing heparin (10 U/ml), and finally with PBS only. NSCs were then trypsinized, centrifuged, and resuspended in PBS containing heparin (10 U/ml) for injections. HPF-labeled NSCs were resuspended to concentrations of 1.25×10^5 NSCs per 2 μ l or 2.5×10^5 NSCs per 2 μ l.

Boyden Chamber Cell Migration Assays

In vitro chemotaxis assays were conducted using 24-well cell culture plates with polycarbonate inserts (8- μ m pore size) (Millipore, Billerica, MA, <http://www.millipore.com>) as described previously [22]. Briefly, conditioned media were prepared by addition of serum-free media to cultured U87 human glioma cells at 75% confluence, followed by incubation (48 hours, 37°C, 6% CO₂). Conditioned media from glioma cells were collected and added to the lower chambers of 24-well plates (600 μ l). Inserts were placed into wells, and a suspension of NSCs in serum-free culture media containing 2% bovine serum albumin (BSA) was added in the upper chamber (10^5 cells per 400 μ l). After incubation of the plates for 4 hours at 37°C, migrated cells were detached from the lower surface of the insert by trypsinization, centrifuged for 5 minutes, and counted using the Guava ViaCount assay (Guava Technologies, Hayward, CA). Only viable cells were included in the data analysis. The Guava ViaCount assay distinguishes between viable and nonviable cells on the basis of the differential permeability of DNA-binding dyes in the ViaCount reagent, and therefore, fluorescence of the dyes allows quantitative assessment of both viable and nonviable cells in suspension. Migration assay controls were as follows: (a) for the negative chemokinesis control, stem cells resuspended in DMEM with 2% BSA were added to the upper and lower chambers; and (b) for the positive control, DMEM with 10% FBS was added to the lower chamber as a chemoattractant. Guava ViaCount assay was also used to assess NSC viability and growth kinetics.

Iron Quantification by Atomic Absorption Spectroscopy and Inductively Coupled Plasma Mass Spectroscopy

HPF-labeled NSCs (2×10^6) were centrifuged (486g) using an Allegra 6R 5810R centrifuge (Beckman Coulter, Fullerton, CA,

<http://www.beckmancoulter.com>), and the pellet was dissolved in concentrated nitric acid (200 μ l; BDH Aristar Plus; VWR International, Visalia, CA, <https://us.vwr.com>) and 30% hydrogen peroxide (200 μ l; BDH) in glass tubes. Tubes were heated to 80°C in a water bath for 10–15 minutes. After digestion was completed, the final volume of the reaction was brought to 2.5 ml with deionized water. Prior to analysis, all samples were centrifuged to remove insoluble materials. A PerkinElmer Analyst 800 atomic absorption spectrometer (S/N 8190) (PerkinElmer Life and Analytical Sciences, Boston, MA, <http://www.perkinelmer.com>) was used to measure the iron content of the specimens in triplicate ($n = 5$ independent experiments). Atomic absorption spectroscopy (AAS) was performed for cell samples. For iron detection in tissue samples, concentrations of iron in brain, liver, and spleen were measured by inductively coupled plasma mass spectrometry (ICP-MS) (American Environmental Testing Laboratory Inc., Burbank, CA, <http://www.aetlab.com>). The tissue samples (0.01–0.2 g) were collected at necropsy. Samples were digested in 4.0 ml of concentrated (69%–70%, $D = 1.42$ g/ml) nitric acid for 2.50 hours, and the final volumes were brought to 500 ml. All digested tissues were filtered with 5A Advantec filter paper (Cole-Parmer, Inc., Vernon Hills, IL, <http://www.coleparmer.com>) and analyzed for iron content.

In Vivo Localization of HB1.F3.CD NSCs to Orthotopic U251T.eGFP.ffluc Glioma Xenografts

To initiate a xenograft model of human glioblastoma, adult *Es1^e/SCID* immunodeficient mice [23] received stereotactic frontal lobe injections of U251T.eGFP.ffluc human glioma cells (2×10^5 cells per 2 μ l of PBS). On day 3 following U251T.eGFP.ffluc engraftment, glioma-bearing mice were injected with HPF-labeled NSCs either intracerebrally, just caudolateral to tumor site (1×10^4 , 5×10^4 , 1×10^5 , or 2×10^5 cells per 2 μ l of PBS) or intravenously (5×10^5 or 2×10^6 cells per 200 μ l of PBS). All mice were magnetic resonance imaged on days 1 and 4 after NSC injection to track the distribution of NSCs in the brain. Mice were euthanized on study day 7, and brain tissue was harvested and postfixed in 4% paraformaldehyde (PFA) for 72–96 hours. Paraffin-embedded histologic sections (10 μ m) were further processed for Prussian blue staining and immunohistochemical staining of enhanced Green Fluorescent Protein (eGFP) to visualize HPF-labeled NSCs and glioma tumor cells, respectively. U251T.eGFP.ffluc cells were modified to stably express eGFP and firefly luciferase (ffluc). HB1.F3.CD NSCs were used for the final safety/toxicity studies (in non-tumor brains). For the NSC migration/distribution glioma studies, they were adenovirally transduced to express a modified human carboxylesterase, hCE1m6 (for conversion of irinotecan to SN-38, a potent topoisomerase inhibitor and anticancer agent) [24].

All animal studies were performed under approved City of Hope (no. 04011) and Children's Hospital of Los Angeles (CHLA) (no. 285) institutional animal care and use committee protocols. Prussian blue staining was performed using the Accustain iron stain kit (Sigma-Aldrich, St. Louis, MO, <http://www.sigmaaldrich.com>) according to the manufacturer's protocol. Adjacent sections were processed for immunoperoxidase-3,3'-diaminobenzidine (DAB) staining with anti-eGFP antibody (ab290; 1:500 dilution; Abcam, Cambridge, MA, <http://www.abcam.com>). Antibody reactivity to eGFP was subsequently detected using a Vectastain ABC Elite kit (Vector Laboratories, Burlingame, CA, <http://www.vectorlabs.com>) and a Peroxidase Substrate Kit (Vector

Laboratories) according to the manufacturer's instructions. Bright-field images of stained sections were obtained using an Automated Cellular Imaging System II (Dako, Carpinteria, CA, <http://www.dako.com>).

Safety and Toxicity Studies of Iron-Labeled NSCs In Vivo

Es1^e/SCID mice were bred and housed at the City of Hope Association for Assessment and Accreditation of Laboratory Animal Care International (AAALAC)-approved animal facility. Using an Omni drill (OMNI Energy Services Corp., Carencro, LA, <http://www.omnienergy.com>) attached to a stereotactic device, one burr hole was made on each side of the skull using the following coordinates: 2 mm lateral (both right and left) and 0.5 mm anterior to bregma. Cells were loaded into a 25- μ l Hamilton syringe with a 30-gauge needle and injected over 2 minutes into each frontal lobe at a depth of 3.3 mm from the surface of the skull. Both burr holes were occluded using bone wax. Adult mice (>8 weeks old) were randomly assigned to four experimental groups, stratified for sex (40%–60% male and 60%–40% female) and weights (females, 22–26 g; males, 24–28 g). Non-tumor-bearing *Es1^e/SCID* mice were injected with HPF-labeled NSCs (in 2 μ l of PBS) in the left and right hemispheres as follows: group 1, 1.25×10^5 NSCs per hemisphere, 2.5×10^5 NSCs total per brain (approximately 0.625 μ g total iron); group 2, 2.5×10^5 NSCs per hemisphere, 5×10^5 NSCs total per brain (approximately 1.25 μ g total iron). Unlabeled NSCs were injected similarly (group 3) but at the high NSC dose only (2.5×10^5 NSCs per hemisphere, 5×10^5 NSCs total per brain) or PBS only (2 μ l) control (group 4) into the frontal lobe. Three time points were assessed: 1 week (10 mice per group), 4 weeks (10 mice per group), and 12 weeks (4 mice per group). Clinical observations of behavior and health were documented twice daily. To histologically assess any potential acute or chronic effects of iron released in the brain, mice were euthanized at week 1, 4, or 12 following isoflurane anesthesia and cardiac puncture for blood withdrawal. A gross necropsy evaluation was performed on the brain, liver, and spleen, including weight, general appearance, and color and presence of obvious tumors or lesions. Blood was taken at the time of tissue harvest and analyzed for iron content and full blood chemistries (RADIL Lab; IDEXX Radil, Sacramento, CA, <http://www.idexbioresarch.com>).

Immunohistochemistry

Harvested brains and organs (liver, spleen, and kidney) were fixed in 4% PFA for 72–96 hours. After fixation, tissues were placed in cassettes, washed three times in distilled water, and kept in 80% ethanol prior to being embedded in paraffin. For brains, 120 sections (10 μ m thick) were cut. Every 10th section was stained by hematoxylin and eosin (H&E). Adjacent sections were processed for Prussian blue staining, according to the manufacturer's protocol (Accustain iron stain kit; Sigma-Aldrich) to visualize iron-labeled cells and counterstained with pararosaniline. To visualize tumor cells, adjacent sections were stained using anti-eGFP antibody (ab290; 1:500 dilution; Proteinase K antigen retrieval; Abcam) and peroxidase-DAB. Bright-field images of stained sections were obtained using an Automated Cellular Imaging System II (Dako). For safety and toxicity experiments, representative brain sections were also examined for the presence of mouse microglia and macrophages using reactivity to anti-ionized calcium-binding adaptor molecule 1 (IBA-1) antibody (019-1974; 1:100 dilution; Wako, Richmond, VA, <http://www.wako.com>).

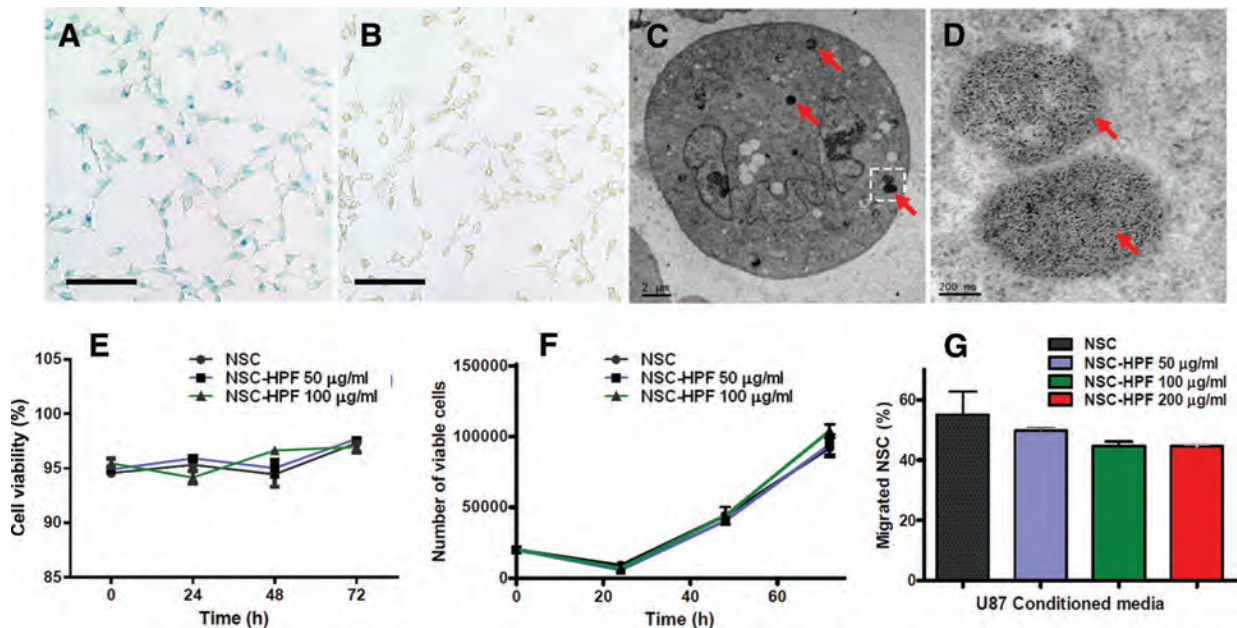


Figure 1. Visualization of iron nanoparticles in NSCs ex post facto and in real-time. **(A):** Prussian blue staining of HPF-labeled NSCs (100 $\mu\text{g/ml}$ ferumoxytol). **(B):** Prussian blue staining of unlabeled NSCs, showing lack of blue staining. **(C):** Transmission electron microscopy image of HPF-labeled NSCs. Red arrows indicate electron-dense particles (ferumoxytol nanoparticles) in endosomes within the cytoplasm. **(D):** Higher magnification image of boxed area in **(C)**. Red arrows indicate punctate appearance of iron particles within endosomes. **(E, F):** Cell viability **(E)** and growth kinetics **(F)** of NSCs were labeled using 0, 50, and 100 $\mu\text{g/ml}$ ferumoxytol in HPF complex and assayed over 72 hours. **(G):** In vitro cell migration to U87 human glioma cell-conditioned media as determined by Boyden chamber assay. Scale bars = 100 μm **(A, B)**, 2 μm **(C)**, and 200 nm **(D)**. Abbreviations: HPF, heparin, protamine sulfate, and ferumoxytol; NSC, neural stem cell.

www.wakousa.com), and examined for the presence of anti-human mitochondria antibody (MAB1273; 1:100 dilution; Millipore) using the Vectastain ABC Elite kit (Vector Laboratories) and the Peroxidase Substrate Kit (Vector Laboratories) according to the manufacturers' instructions; all sections were then counterstained with hematoxylin.

Magnetic Resonance Imaging

Mice were anesthetized with isoflurane throughout the imaging procedure. Mice were inserted in the prone position into a small animal MRI scanner (PharmaScan 300; Bruker BioSpin Division, Billerica, MA, <http://www.bruker.com>) 7T magnet using the 19-mm inner diameter transmit receive coil. ParaVision 4.0 scanner software (Bruker BioSpin, The Woodlands, TX, <http://www.bruker.com/paravision>) was set to use the Rapid Acquisition with Relaxation Enhancement (RARE) spin echo sequence for fast T2-weighted imaging (TE 50, TR 3000, RARE Factor 8) with a 256 \times 256 in-plane matrix and a 2.56-cm field of view. After being scanned, mice were gently warmed on a thermostatically controlled heating pad until they were awake enough to be returned to their home cage. MR images were reconstructed at native resolution. For each mouse, we acquired 22 axial images with 0.4-mm-thick slices and a 0.02-mm gap between slices on days 1 and 4 post-NSC injection. This produced a 0.1 \times 0.1 mm per pixel in-plane resolution with an effective slice thickness of 0.42 mm. DICOM data were stored in the small animal imaging PACS server and processed using the Mayo ANALYZE (AnalyzeDirect, Inc., Overland Park, KS, <http://www.analyzedirect.com>) and OsiriX (Open-Source Software for Navigating in Multidimensional DICOM Images) image analysis software packages [25].

Statistical Analysis

Statistical analyses of data originating from the safety and toxicity studies for submission of an amendment to existing Investigational New Drug (IND) application #14041 (ClinicalTrials.gov identifier NCT01172964) to the FDA were performed using R [26]. All other analyses were performed with GraphPad Prism (v.6.0b for Mac OS X; GraphPad Software, Inc., San Diego, CA, <http://www.graphpad.com>).

RESULTS

Labeling of NSCs With Ferumoxytol

In this study, we used the *v-myc*-immortalized human clonal HB1.F3.CD NSC line, which is genetically and functionally stable, nontumorigenic, and minimally immunogenic [20, 21]. To determine whether the characteristics of these NSCs are affected by labeling with ferumoxytol, we performed comparative tests between unlabeled and ferumoxytol (HPF)-labeled HB1.F3.CD NSCs. Ferumoxytol (F), when combined with protamine sulfate (P) and heparin (H) at a ratio of 2 units/ml H to 40 $\mu\text{g/ml}$ P to 100 $\mu\text{g/ml}$ F (HPF complex) and used for the labeling of NSCs, had greater than 95% labeling efficiency (Fig. 1A). In vitro Prussian blue staining demonstrated that iron was present within the cytoplasm of HPF-labeled NSCs, whereas no staining was detected in unlabeled control cells (Fig. 1B). Electron microscopy showed that iron oxide nanoparticles were localized in subcellular structures, likely endosomes, and were not diffusely distributed throughout the cytoplasm or on the surface of the NSCs (Fig. 1C, 1D). The concentration of iron per cell for NSCs, as determined by AAS, was 2.46 ± 1.60 pg per cell (mean \pm SD, $n = 5$), similar to

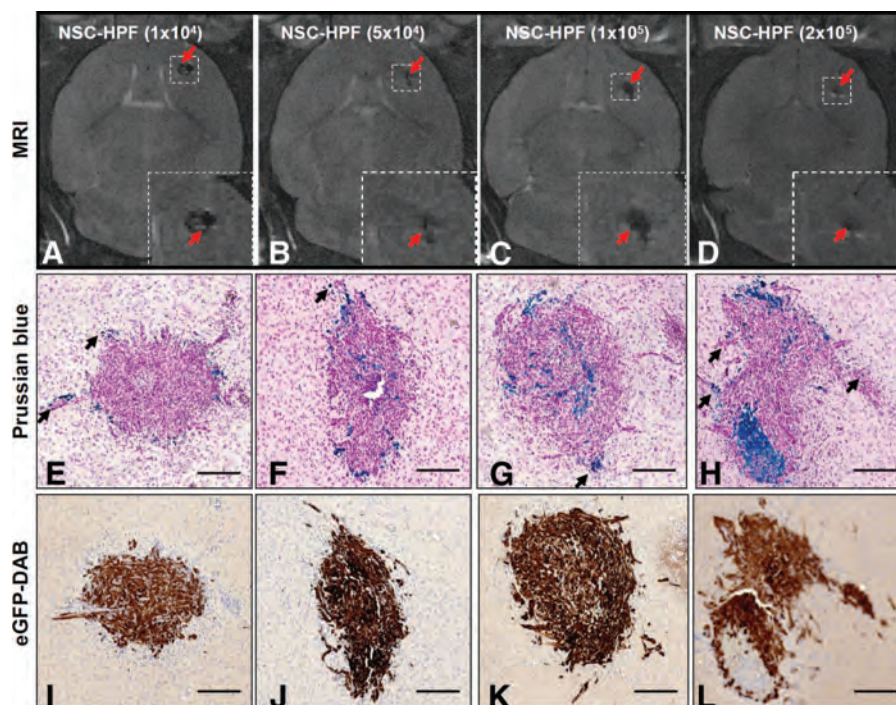


Figure 2. Intracerebrally injected HPF-labeled NSCs migrate and distribute to orthotopic U251T.eGFP.ffluc gliomas. Intracerebral xenografts in mice were established by stereotactic implantation of 2×10^5 U251T.eGFP.ffluc human glioma cells into the right frontal hemisphere. Three days later, HPF-labeled NSCs (1×10^4 , 5×10^4 , 1×10^5 , or 2×10^5) were injected caudolateral to the tumor. (A–D): T2-weighted magnetic resonance images of mouse brains obtained 4 days after NSC administration. Red arrows indicate hypointense (black) signals associated with HPF-labeled NSCs. Boxed areas are magnified in the image insets. (E–H): Prussian blue stained and pararosaniline-counterstained brain tumor sections with NSCs (black arrows). HPF-labeled NSCs that migrated to tumor are stained blue. (I–L): Adjacent brain tumor sections immunohistochemically stained for eGFP to identify tumor cells (brown), counterstained with hematoxylin. Scale bars = 200 μ m. Abbreviations: DAB, 3,3'-diaminobenzidine; eGFP, enhanced Green Fluorescent Protein; HPF, heparin, protamine sulfate, and ferumoxytol; MRI, magnetic resonance imaging; NSC, neural stem cell.

values recently reported [18]. Important for future clinical use, no significant biologically relevant differences were detected in cell viability, growth kinetics, or tumor tropism of HPF-labeled NSCs (concentrations of ferumoxytol in the HPF complex were 50 or 100 μ g/ml) when compared with unlabeled NSCs over 4 days in culture (Fig. 1E–1G). Statistical analysis of the growth curves of the cells unlabeled or labeled with 50 or 100 μ g/ml HPF revealed no significant differences using a two-tailed *t* test with *p* values ranging from .11 to .15 for all groups (Fig. 1F).

Intracerebrally Administered HPF-Labeled NSCs Localize to Orthotopic Glioma Xenografts

Orthotopic glioma xenografts were generated by injecting U251T.eGFP.ffluc human glioma cells (2×10^5) into the right frontal hemisphere of adult *Es1^e/SCID* mice. Three days later, HPF-labeled NSCs were administered just caudolateral to the tumor site in escalating doses (1×10^4 , 5×10^4 , 1×10^5 , 2×10^5 NSCs; *n* = 8 mice per dose). NSC migration and distribution around and within glioma xenografts was monitored by MRI on days 1 and 4 post-NSC injection (Fig. 2A–2D; day 4 MRI). Mice received preinterventional MR images before NSC injection (day 0) (data not shown). Mice were euthanized 7 days after tumor implantation, and brain tissues were processed for histological examination. H&E staining of brain sections revealed compact tumor nodules, predominantly located in the deep cortex and caudate-putamen, ranging in size between 0.6 and 1 mm. Prussian blue staining showed HPF-labeled NSCs at the tumor site and dispersed within the tumor nodules (Fig. 2E–2H). NSCs were

also present in peripheral areas of the tumor, including infiltrating tumor cell bundles (Fig. 2E–2H, Prussian blue-stained NSCs). The injection site for HPF-labeled NSCs could often be identified as a distinct and compact cellular focus located next to the tumor site. Tumor sites were confirmed by immunostaining for enhanced green fluorescent protein (eGFP) (Fig. 2I–2L). Alternatively, HPF-NSCs were injected intracranially, contralateral to the tumors. Four days after HPF-NSC injection (study day 7), brains were harvested, sectioned, and stained with Prussian blue to detect HPF-labeled NSCs at infiltrating glioma sites (supplemental online Fig. 3).

Intravenously Administered HPF-Labeled NSCs Localize to Orthotopic Glioma Xenografts

Glioma xenografts were generated by implanting 2×10^5 U251T.eGFP.ffluc human glioma cells into the right frontal hemisphere of *Es1^e/SCID* mice. HPF-labeled NSCs (5×10^5 or 2×10^6) were injected into the tail vein of mice 3 days after tumor engraftment. Hypointense (dark) voxels on T2-weighted MR images were detected in the brain on day 4 after intravenous injection of HPF-labeled NSCs (Fig. 3A, 3D). Tumor localization of NSCs was confirmed by Prussian blue staining of tissue sections from brain harvested 4 days after NSC injection (Fig. 3B, 3E). Glioma cells were detected by eGFP immunohistochemistry on adjacent sections, which identified the main tumor (size range, 0.6–1 mm), as well as infiltrating tumor cells (Fig. 3C, 3F). Prussian blue-stained NSCs were primarily detected in the peripheral areas of tumors and in association with invasive glioma cells (Fig.

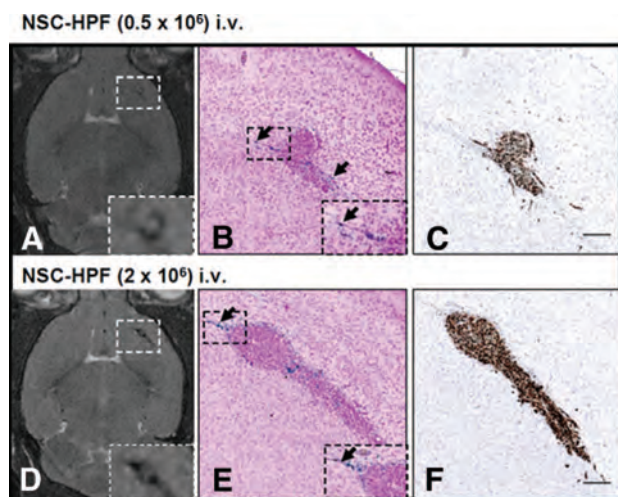


Figure 3. Intravenously injected HPF-labeled NSCs migrate and distribute to orthotopic glioma xenografts. Intracerebral xenografts in mice were established by stereotactic implantation of 2×10^5 U251.eGFP.fluc human glioma cells into the right frontal hemisphere. Three days later, specified numbers of HPF-labeled NSCs (5×10^5 , 2×10^6) were injected intravenously via the tail vein. (A, D): T2-weighted MRIs of mouse brains obtained 4 days after 0.5×10^6 (A) or 2×10^6 (D) HPF-labeled NSCs were administered intravenously. Boxed areas are magnified in the image insets. (B, E): Prussian blue staining of brain sections of mice euthanized immediately after MRI. Arrows indicate HPF-labeled NSCs that migrated to U251.eGFP.fluc glioma xenografts. Boxed areas are magnified in the image insets. (C, F): Brain sections adjacent to the sections in (B) and (E) stained with anti-enhanced green fluorescence protein (eGFP) antibodies to identify tumor nodules and invasive cells (brown). Sections were counterstained with hematoxylin. Scale bars = $200 \mu\text{m}$. Abbreviations: HPF, heparin, protamine sulfate, and ferumoxytol; NSC, neural stem cell.

3B, 3E, black arrows). Foamy macrophages (identified morphologically) were rarely seen in close association with tumor cells and were not stained by Prussian blue.

Biodistribution and Safety of HPF-Labeled NSCs in the CNS

To demonstrate the safety of the HPF-labeled NSCs, non-tumor-bearing male and female *Es1^e/SCID* mice were injected with HPF-labeled or unlabeled NSCs in the left and right frontal hemispheres (1.25×10^5 NSCs per hemisphere, 2.5×10^5 NSCs total per brain, or 2.5×10^5 NSCs per hemisphere, 5×10^5 NSCs total per brain). *Es1^e/SCID* mice are compatible hosts for human NSCs. The purpose of labeling with ferumoxytol is to allow for MRI tracking of NSC migration and distribution following injection into the patients. At present, the lower level of detection is 10–30 iron-labeled NSCs in a typical 7-Tesla mouse imaging voxel. Extrapolating from this data to a typical 3-Tesla patient imaging voxel, the lower limit of visualization is predicted to be as few as 500–1,000 iron-labeled NSCs. We estimated a loading dose of 2.5 pg of iron per NSC. Therefore, the amounts of iron used in this study were approximately $0.625 \mu\text{g}$ of total iron for 2.5×10^5 NSCs, and $1.25 \mu\text{g}$ of total iron for 5×10^5 NSCs. Based on an average brain mass of 0.5 g for mice and 1,500 g for humans, the human dose equivalents would be 1.875 mg and 3.75 mg of total iron injected for the lower and higher doses, respectively. The proposed amounts of iron delivered via HPF-labeled NSCs in human clinical trials will be approximately 125 and 250 μg of iron, for doses of 5×10^7 and 1×10^8 HPF-labeled NSCs,

respectively. Therefore the doses tested in mice were 7.5–30-fold higher than the proposed doses in humans. Control groups received similar injections of unlabeled NSCs (at the highest dose of 2.5×10^5 NSCs per hemisphere) or PBS only. Mice were separated into three groups euthanized at week 1 ($n = 10$ per group), week 4 ($n = 10$ per group), or week 12 ($n = 5$ per group) after NSC injections, constituting acute, mid, and late effects groups, respectively. Mouse behavior and health were monitored and recorded twice daily. Brain tissue was histologically examined for evidence of any acute or long-term effects of iron release at 1, 4, and 12 weeks after NSC injection (Fig. 4). H&E and Prussian blue staining of $10\text{-}\mu\text{m}$ paraffin-embedded brain sections revealed 1.2–1.8 mm foci of architectural distortion that were associated with mild hypercellularity and involved the cortex and caudate-putamen (Fig. 4A–4D). Such foci were composed predominantly of foamy macrophages and cells that had a moderate amount of amphiphilic cytoplasm, consistent with the presence of NSCs. There was no evidence of local neurotoxicity, such as cystic disruption, associated with the injection of HPF-labeled or unlabeled NSCs, and no dilation of ventricles or anoxic/ischemic changes (Fig. 4A–4D). The presence of HPF-labeled NSCs in the brain was confirmed by Prussian blue staining (Fig. 4A–4D) and anti-human mitochondria immunohistochemistry (Fig. 4E–4G). NSCs were not seen distant from the injection site in the brain or in other organs (liver and spleen) as assessed by anti-human mitochondria immunohistochemistry [1]. To detect mouse microglia and macrophages that reacted to the injection of HPF-labeled or unlabeled NSCs, adjacent slides were stained with IBA-1 antibodies. IBA-1 is a 17-kDa calcium binding protein that is not normally expressed in brain but is highly induced upon inflammatory signals in macrophages and microglia. IBA-1 reactivity was present near the injection tracts and diminished with distance from these sites in mice that received labeled or unlabeled NSCs (Fig. 4I–4L). H&E and Prussian blue staining of liver and spleen showed no evidence of abnormal iron deposition or other histologically identifiable diagnostic abnormalities associated with injection of HPF-labeled, unlabeled NSCs or PBS vehicle control 7 days after NSC injections (supplemental online Fig. 1; $n = 10$ mice per group).

Mid-term (4 weeks) and long-term (12 weeks) safety studies using a similar study protocol revealed no iron-associated toxicities in the brain (supplemental online Fig. 2). Iron deposits detected by Prussian blue staining were localized to injection sites, decreased over time, and appeared to have resulted from scavenging by macrophages. Because some of these Prussian blue-positive nodes were present near injection sites of mice that did not receive NSCs or iron, we attribute these areas of positive staining to macrophage/microglia scavenging of iron from heme and the degradation products released from red blood cells at the site of injury incurred as a result of the injection. No mid- or long-term effects of HPF-NSC administration were detected in the brain or other organs (supplemental online Figs. 1, 2). Use of anti-human mitochondria antibodies to identify NSCs 4 weeks post-NSC injection revealed only a few viable cells (supplemental online Fig. 2), and no NSCs were detected at week 12 (Fig. 4H). Mouse microglia reactions were evaluated at weeks 4 and 12 after NSC injections (Fig. 4K, 4L). After 4 weeks, IBA-1 staining (Fig. 4K) appeared to decrease compared with week 1 (Fig. 4J), and a further decrease was seen at 12 weeks (Fig. 4L) that approached background levels. No significant differences were

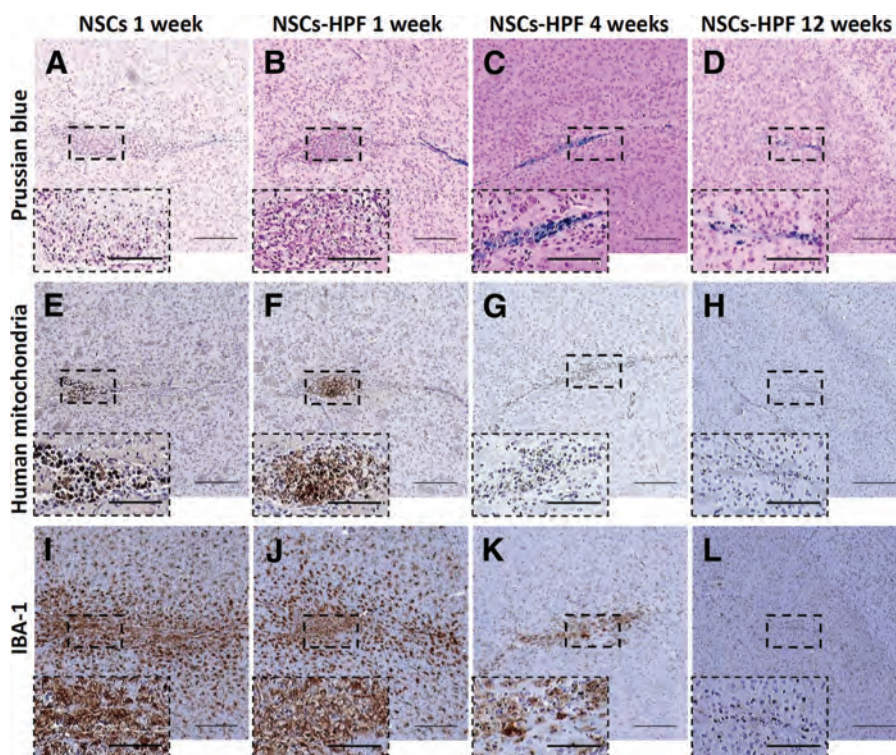


Figure 4. Histological analysis of brain sections from mice euthanized at 1 week (A, B, E, F, I, J), 4 weeks (C, G, K), and 12 weeks (D, H, L) after receiving unlabeled (A, E, I) or HPF-labeled (B–D, F–H, J–L) HB1.F3.CD NSCs injected intracerebrally. (A–D): Prussian blue staining revealed iron-positive cells in the vicinity of the injections sites (boxed) in the brain. (E–H): Immunohistochemical detection of human mitochondria-positive NSCs (boxed) in the brain sections of mice (boxed regions are magnified in the image insets). (I–L): Immunohistochemistry detection of the activated microglia and macrophages in areas of local gliosis in the vicinity of the injection sites using IBA-1 antibodies. Scale bars = 200 μm (main panels) and 100 μm (insets). Abbreviations: HPF, heparin, protamine sulfate, and ferumoxylol; IBA-1, ionized calcium-binding adaptor molecule 1; NSC, neural stem cell.

seen in mouse microglia reactions to HPF-labeled NSCs compared with unlabeled NSCs. H&E and Prussian blue staining of sections prepared from PFA-fixed and paraffin-embedded liver and spleen showed no evidence of excess iron deposition compared with control mice that received unlabeled NSCs or PBS only (supplemental online Fig. 3).

There were no diagnostic abnormalities associated with injection of HPF-labeled or unlabeled NSCs or PBS vehicle control at 4 or 12 weeks post-NSC injection (supplemental online Fig. 2A–2H; $n = 10$ mice per group). Only the spleen showed iron staining, as assessed by Prussian blue, and this staining was physiological because the endogenous levels of iron are high in this organ [27]. Iron content of liver, spleen, and brain were measured by ICP-MS at the contract laboratory. The iron content values for organs were transformed using a natural log distribution and compared using a Student's t test allowing for unequal variances (Table 1). At 1 week, there was an increase in brain iron content consistent with the amount given; that is, the iron levels in mice receiving 2.5×10^5 HPF-labeled NSCs and 5.0×10^5 HPF-labeled NSCs were significantly higher than in mice from the group that received NSCs with no iron. However, only the iron content of brains from mice receiving the high dose of NSCs had 95% confidence limits entirely outside of the 0.2 range. Furthermore, these differences disappeared at 12 weeks. Mice that received HPF-labeled NSCs did not exhibit greater Prussian blue staining. Finally, intracerebral administration of HPF-labeled NSCs did not cause clinical or behavioral changes in mice at any time, and no physiologically significant hematological or blood

Table 1. Iron content of organs

Group (sample)	Sample size	Missing	Mean ($\mu\text{g/g}$ of tissue)	Standard deviation
G1 (brain)	10	0	17.22	3.39
G2 (brain)	10	0	20.48	3.00
G3 (brain)	10	0	14.16	2.01
G4 (brain)	10	0	14.34	3.18
G1 (liver)	10	0	108.72	36.35
G2 (liver)	10	0	137.09	33.66
G3 (liver)	10	0	127.91	25.24
G4 (liver)	10	0	142.58	33.07
G1 (spleen)	10	0	701.54	267.96
G2 (spleen)	10	0	602.16	208.96
G3 (spleen)	10	0	957.41	383.63
G4 (spleen)	10	0	854.96	440.26

chemistry abnormalities were found (data not shown). The behavior and health of the mice were monitored and recorded Monday through Saturday. The rate of clinical observations requiring euthanasia was 0, with 95% exact upper and lower Clopper-Pearson confidence limits of 0 and 0.31 for each treatment group based on a sample size of 10. The results for all four groups were the same for the 1-week study, and similar results were obtained for the 4- and 12-week studies. A gross necropsy evaluation was performed and recorded on brain, liver, and spleen, including weight, general appearance, color, and obvious tumors or lesions. Gross necropsy data showed no abnormalities. Blood, taken at the time of euthanasia, was analyzed for full blood chemistry and hematology (data not shown). No deaths or

adverse effects attributable to the administration of HPF-labeled or unlabeled NSCs were observed.

DISCUSSION

As with any cell-based therapy, the efficacy of an NSC-mediated cancer treatment approach depends on the safety and ability of NSCs to adequately target and distribute throughout tumor sites [28–30]. To advance the use of NSCs as therapeutic agents, we used noninvasive MRI to monitor spatiotemporal migration of NSCs to tumor sites. Recent studies have shown that iron-labeled cells can be tracked by susceptibility-sensitive T2 and T2*-weighted MRI [11, 31, 32]. We have previously demonstrated that the combination of ferumoxides with protamine sulfate can be used to label NSCs for this purpose [13]. Thu et al. reported protocols for iron labeling of different types of cells with HPF, the components of which are all approved for clinical use by the FDA [18]. In the current study, we optimized this HPF cell-labeling protocol for use in the HB1.F3.CD NSC line to enable MRI tracking of HPF-labeled NSCs. NSCs labeled using the HPF protocol are viable and proliferative, and they retain their tumor tropism in vitro. In vivo, we demonstrated NSC localization to orthotopic human glioma via both intracerebral and intravenous routes of administration. Furthermore, we visualized the distribution of HPF-labeled NSCs in vivo by MRI and confirmed these observations by histological methods.

In the current studies, we also established the safety of iron-loaded NSCs when given to normal non-tumor-bearing *Es1^c/SCID* mice. Three independent lines of evidence suggest that the additional iron load of HPF-labeled NSCs was nontoxic in the host, both acutely and long-term. First, based on quantitative assessment, the amount of iron delivered to the host was minimal compared with many naturally occurring (i.e., by ingestion) or exogenous sources of iron (e.g., blood transfusions or iron therapy in chronic kidney disease), suggesting that no organ should show any appreciable increased uptake or deposition of iron. Second, the NSCs themselves were not measurably affected by the intracellular HPF labeling and are therefore unlikely to harm tissues in which they reside. Third, hosts that received iron-labeled NSCs did not exhibit signs or symptoms of toxicity or illness consistent with other published studies [33–36]. Therefore, effects on the host are minimal or undetectable and of no negative clinical impact. Regarding the fate of transplanted NSCs, our previous data showed that the HB1.F3.CD NSCs stop dividing within 48–72 hours after transplantation as indicated by lack of staining with the cell proliferation markers Ki67 and proliferating cell nuclear antigen. Thus, a likely explanation for the decreased Prussian blue staining in the current study (Fig. 4) may be that the NSCs die (which is consistent with the observed decrease in immunohistochemical staining for human mitochondria), resulting in loss of intracellular iron. The dead NSCs and the ferumoxytol nanoparticles may be phagocytosed by microglia and macrophages that are present at the NSC injection site (Fig. 4) over time. Of note, when ferumoxytol was injected intracerebrally into rats in another study, the half-life of the ferumoxytol signal was 3–10 weeks (depending on the dose injected) as detected by T2-weighted MRI [37]. This is consistent with our current data on the observed decrease in intensity of the Prussian blue iron staining over the course of 1–12 weeks (Fig. 4). It should be noted that a very small percentage of the transplanted NSCs may differentiate into neurons or glial cells, which may retain the

ferumoxytol nanoparticles for a longer time, prior to being metabolized [20].

As noted above, after iron-labeled NSCs die, the remaining iron is likely metabolized by normal processes associated with physiologically normal iron clearance mechanisms. Macrophages can store excess iron in endosomes or may export it across the cell membrane to tissues where it is needed or to the liver for further metabolism. The lack of acute toxicity reported in cases where iron labeling has already been used clinically supports our observation that it is being metabolized by normal processes and is well within physiologically tolerated levels [38–40]. Pawelczyk et al. reported on the effect of labeling cells with ferumoxides on cellular iron metabolism [40]. Ferumoxytol has the same chemical structure as iron oxide crystal and would be metabolized identically to ferumoxides by cells. In response to ferumoxide loading into endosomes, the cells downregulate transferrin gene expression and protein and upregulate ferritin gene expression and protein levels [40]. Iron from the nanoparticles can be released into the intracellular compartment and participate in cellular iron metabolism [41]. Intravenously injected ferumoxytol shows uptake in spleen and bone marrow, whereas intracranial injection of ferumoxytol shows slow clearance from the brain based on MRI [17]. Iron metabolism is a fundamental physiological process in humans, both for the clearance of dead cells and during hematopoiesis. Iron-loading methods described in the literature indicate that labeling cells with iron increases their iron content by 1–15 pg per cell [5]. Our cell labeling procedure resulted in approximately 2.5 pg of iron per NSC and an average total iron load to the brain of 0.625 and 1.25 μg for the lower and higher NSC doses, respectively. A similar concentration of iron per cell was reported in a previous study in which NSCs were labeled with HPF complexes [18]. Thus, the amount of iron contained in the proposed doses of NSCs (10 million or 50 million NSCs; clinical trial NCT01172964) for a human patient is substantially less than the amount of iron contained in 0.1 ml of blood. Therefore, we conclude that HPF-loaded NSCs will not add a significant iron load to the patient. Importantly, we observed the normal recovery of mouse brain tissue in the vicinity of the injection sites over a 12-week period. Specifically, areas of gliosis as evidenced by the increased presence of activated macrophages and microglia subsided to levels found in untreated regions farther away from the injection sites in mice that received either both ferumoxytol-loaded or unlabeled NSCs. There was no observable difference in the level of gliosis or recovery between any of the treatment groups. Histochemical detection of iron revealed the expected differences between mice that did or did not receive iron at the early time points, whereas over time, there was no observable difference in iron deposition between groups, suggesting that normal physiological processes acted to scavenge any added iron. We interpret these observations to mean that the physiological reaction to ferumoxytol-containing cells is no worse than the reaction to the wound injury sustained from the surgical procedures. Furthermore, since ferumoxytol-labeled NSCs retain their migratory capabilities when administered by either the intracerebral or the intravenous (i.v.) route of administration, further development and optimization of the i.v. route is

warranted since it may provide an option for nonsurgical patients and make multiple rounds of NSC treatment more feasible and cost-effective.

CONCLUSION

In conclusion, we propose that ferumoxytol labeling is an effective cell-tracking method that is safe for clinical use, contributing little to the risk side of a given risk/benefit analysis. Our ongoing FDA-approved clinical trial focuses on the use of NSCs as delivery vehicles for enzyme/prodrug treatment of recurrent glioma patients [1]. The broader objective of the current study was to develop a safe and effective strategy to monitor the transplanted NSCs over time by MRI. The results reported herein formed the basis of an amendment submitted to the FDA that was approved for human use in April 2012. To date, three patients have been treated with HPF-labeled NSCs, and the ensuing analyses will be published upon completion of the study.

ACKNOWLEDGMENTS

We acknowledge the technical support of Elizabeth Garcia, Soraya Aramburo, and Valerie V. Valenzuela; the technical expertise and advice of Sofia Loera of the Pathology Core and Drs. Marcia Miller and Zhuo Li in the Electron Microscopy Core (supported by funding from Naval Research Grant N00014-02-1 0958); and the editorial assistance of Dr. Keely L. Walker (City of Hope). We thank Catherine Matsumoto and Katherine Furness of the Office of IND Development and Research Affairs (City of Hope) for their assistance with preparation of the IND amendment to the FDA. We also thank the Imaging Group at CHLA, especially Gevorg Karapetyan, Ira Harutyunyan, Anahit Hovsepian, and Seda Mkhitarian. This work was supported by funding from the California Institute for Regenerative Medicine (DR1-01421), NIH/National Institute of Neurological Disorders and

Stroke (U01 NS069997), NIH/National Cancer Institute (P30-CA033572), the Rosalinde and Arthur Gilbert Foundation, and STOP Cancer.

AUTHOR CONTRIBUTIONS

M.G.: data analysis including MRI and histopathology, lead author for manuscript preparation; J.A.F.: protocol development for HPF labeling, consultation on toxicity studies; M.D.: provision of histopathology analysis and reports on all stained tissue sections; V.K.: performance and supervision of animal experiments, xenogen and MRI imaging; M.M.G.: performance of immunocytochemistry, optical imaging and data collection; A.J.A.: performance of MRI analysis, data analysis, manuscript preparation; M.Z.M., Y.A., K.A.H.: performance and analysis of all in vitro studies; L.Y.G.: data and statistical analysis, preparation of documents for IND amendment to FDA, and manuscript preparation; J.N., C.E.B., M.E.B.: assistance in study design, immunochemistry and data analysis, manuscript preparation; M.S.B.: lead statistician, statistical analysis of all data submitted to the FDA; M.S.L.: manuscript review and technical consultation; S.U.K.: provision of HB1.F3.CD neural stem cells; K.S.A. and R.A.M.: principal investigators, planning, design, and supervision of experiments, data analysis and interpretation, preparation of final manuscript, FDA IND 14041 amendment submission.

DISCLOSURE OF POTENTIAL CONFLICTS OF INTEREST

A.J.A. is an uncompensated Board Member and Chief Operating Officer of TheraBiologics. K.S.A. is an uncompensated Board Member, Chief Scientific Officer, and shareholder of TheraBiologics. R.A.M. is an uncompensated Board Member of TheraBiologics. L.Y.G. is a cofounder, shareholder, and Scientific Director of Keren Pharmaceuticals.

REFERENCES

- 1 Aboody KS, Najbauer J, Metz MZ et al. Neural stem cell-mediated enzyme/prodrug therapy for glioma: Preclinical studies. *Sci Transl Med* 2013;5:184ra59.
- 2 Gilad AA, Walczak P, McMahon MT et al. MR tracking of transplanted cells with "positive contrast" using manganese oxide nanoparticles. *Magn Reson Med* 2008;60:1-7.
- 3 Bhujwala ZM, Artemov D, Natarajan K et al. Reduction of vascular and permeable regions in solid tumors detected by macromolecular contrast magnetic resonance imaging after treatment with antiangiogenic agent TNP-470. *Clin Cancer Res* 2003;9:355-362.
- 4 Sims TL Jr., Hamner JB, Bush RA et al. Neural progenitor cell-mediated delivery of interferon beta improves neuroblastoma response to cyclophosphamide. *Ann Surg Oncol* 2008;15:3259-3267.
- 5 Frank JA, Anderson SA, Kalsih H et al. Methods for magnetically labeling stem and other cells for detection by in vivo magnetic resonance imaging. *Cytotherapy* 2004;6:621-625.
- 6 Frank JA, Kalish H, Jordan EK et al. Color transformation and fluorescence of Prussian blue-positive cells: Implications for histologic verification of cells labeled with superparamagnetic iron oxide nanoparticles. *Mol Imaging* 2007;6:212-218.
- 7 Corot C, Robert P, Idee JM et al. Recent advances in iron oxide nanocrystal technology for medical imaging. *Adv Drug Deliv Rev* 2006;58:1471-1504.
- 8 Chien LY, Hsiao JK, Hsu SC et al. In vivo magnetic resonance imaging of cell tropism, trafficking mechanism, and therapeutic impact of human mesenchymal stem cells in a murine glioma model. *Biomaterials* 2011;32:3275-3284.
- 9 Balakumaran A, Pawelczyk E, Ren J et al. Superparamagnetic iron oxide nanoparticles labeling of bone marrow stromal (mesenchymal) cells does not affect their "stemness." *PLoS One* 2010;5:e11462.
- 10 Artemov D, Mori N, Ravi R et al. Magnetic resonance molecular imaging of the HER-2/neu receptor. *Cancer Res* 2003;63:2723-2727.
- 11 Arbab AS, Pandit SD, Anderson SA et al. Magnetic resonance imaging and confocal microscopy studies of magnetically labeled endothelial progenitor cells trafficking to sites of tumor angiogenesis. *STEM CELLS* 2006;24:671-678.
- 12 Yun J, Sonabend AM, Ulasov IV et al. A novel adenoviral vector labeled with superparamagnetic iron oxide nanoparticles for real-time tracking of viral delivery. *J Clin Neurosci* 2012;19:875-880.
- 13 Thu MS, Najbauer J, Kendall SE et al. Iron labeling and pre-clinical MRI visualization of therapeutic human neural stem cells in a murine glioma model. *PLoS One* 2009;4:e7218.
- 14 Wu X, Hu J, Zhou L et al. In vivo tracking of superparamagnetic iron oxide nanoparticle-labeled mesenchymal stem cell tropism to malignant gliomas using magnetic resonance imaging. Laboratory investigation. *J Neurosurg* 2008;108:320-329.
- 15 Wu YJ, Muldoon LL, Varallyay C et al. In vivo leukocyte labeling with intravenous ferumoxides/protamine sulfate complex and in vitro characterization for cellular magnetic resonance imaging. *Am J Physiol Cell Physiol* 2007;293:C1698-C1708.
- 16 Weinstein JS, Varallyay CG, Dosa E et al. Superparamagnetic iron oxide nanoparticles: Diagnostic magnetic resonance imaging and potential therapeutic applications in neurooncology and central nervous system inflammatory pathologies, a review. *J Cereb Blood Flow Metab* 2010;30:15-35.

- 17 Neuwelt EA, Varallyay CG, Manninger S et al. The potential of ferumoxytol nanoparticle magnetic resonance imaging, perfusion, and angiography in central nervous system malignancy: A pilot study. *Neurosurgery* 2007;60:601–611, discussion 611–602.
- 18 Thu MS, Bryant LH, Coppola T et al. Self-assembling nanocomplexes by combining ferumoxytol, heparin and protamine for cell trafficking by MRI. *Nat Med* 2012;18:463–467.
- 19 Spinowitz BS, Kausz AT, Baptista J et al. Ferumoxytol for treating iron deficiency anemia in CKD. *J Am Soc Nephrol* 2008;19:1599–1605.
- 20 Kim SU. Human neural stem cells genetically modified for brain repair in neurological disorders. *Neuropathology* 2004;24:159–171.
- 21 Kim SU, Nakagawa E, Hatori K et al. Production of immortalized human neural crest stem cells. *Methods Mol Biol* 2002;198:55–65.
- 22 Gutova M, Najbauer J, Frank RT et al. Urokinase plasminogen activator and urokinase plasminogen activator receptor mediate human stem cell tropism to malignant solid tumors. *STEM CELLS* 2008;26:1406–1413.
- 23 Morton CL, Iacono L, Hyatt JL et al. Activation and antitumor activity of CPT-11 in plasma esterase-deficient mice. *Cancer Chemother Pharmacol* 2005;56:629–636.
- 24 Wierdl M, Tsurkan L, Hyatt JL et al. An improved human carboxylesterase for enzyme/prodrug therapy with CPT-11. *Cancer Gene Therapy* 2008;15:183–192.
- 25 Rosset A, Spadola, L, Ratib O. OsiriX: An open-source software for navigating in multi-dimensional DICOM images. *J Digit Imaging* 2004;17:205–216.
- 26 R Core Development R: A language and environment for statistical computing. 2013.
- 27 Wang D, Shi L, Wang YX et al. Color quantification for evaluation of stained tissues. *Cytometry A* 2011;79:311–316.
- 28 Aboody K, Capela A, Niazi N et al. Translating stem cell studies to the clinic for CNS repair: Current state of the art and the need for a Rosetta Stone. *Neuron* 2011;70:597–613.
- 29 Aboody KS, Bush RA, Garcia E et al. Development of a tumor-selective approach to treat metastatic cancer. *PLoS One* 2006;1:e23.
- 30 Aboody KS, Najbauer, J, Danks MK. Stem and progenitor cell-mediated tumor selective gene therapy. *Gene Ther* 2008;15:739–752.
- 31 Arbab AS, Rad AM, Iskander AS et al. Magnetically-labeled sensitized splenocytes to identify glioma by MRI: A preliminary study. *Magn Reson Med* 2007;58:519–526.
- 32 Arbab AS, Wilson LB, Ashari P et al. A model of lysosomal metabolism of dextran coated superparamagnetic iron oxide (SPIO) nanoparticles: Implications for cellular magnetic resonance imaging. *NMR Biomed* 2005;18:383–389.
- 33 Arbab AS, Yocum GT, Wilson LB et al. Comparison of transfection agents in forming complexes with ferumoxides, cell labeling efficiency, and cellular viability. *Mol Imaging* 2004;3:24–32.
- 34 Amsalem Y, Mardor Y, Feinberg MS et al. Iron-oxide labeling and outcome of transplanted mesenchymal stem cells in the infarcted myocardium. *Circulation* 2007;116:138–145.
- 35 Delcroix GJ, Jacquart M, Lemaire L et al. Mesenchymal and neural stem cells labeled with HEDP-coated SPIO nanoparticles: In vitro characterization and migration potential in rat brain. *Brain Res* 2009;1255:18–31.
- 36 Kim HS, Oh SY, Joo HJ et al. The effects of clinically used MRI contrast agents on the biological properties of human mesenchymal stem cells. *NMR Biomed* 2010;23:514–522.
- 37 Muldoon LL, Sandor M, Pinkston KE et al. Imaging, distribution, and toxicity of superparamagnetic iron oxide magnetic resonance nanoparticles in the rat brain and intracerebral tumor. *Neurosurgery* 2005;57:785–796, discussion 785–796.
- 38 Zhu J, Zhou, L, XingWu F. Tracking neural stem cells in patients with brain trauma. *N Engl J Med* 2006;355:2376–2378.
- 39 Toso C, Vallee JP, Morel P et al. Clinical magnetic resonance imaging of pancreatic islet grafts after iron nanoparticle labeling. *Am J Transplant* 2008;8:701–706.
- 40 Pawelczyk E, Arbab AS, Pandit S et al. Expression of transferrin receptor and ferritin following ferumoxides-protamine sulfate labeling of cells: Implications for cellular magnetic resonance imaging. *NMR Biomed* 2006;19:581–592.
- 41 Weissleder R, Stark DD, Engelstad BL et al. Superparamagnetic iron oxide: Pharmacokinetics and toxicity. *AJR Am J Roentgenol* 1989;152:167–173.



See www.StemCellsTM.com for supporting information available online.